Comparison of Two Numerical Schemes of the Fractional Chemical Model

Khaled M. Saad[a,b]

[a]Department of Mathematics, College of Arts and Sciences ,
Najran University, Najran, Kingdom of Saudi Arabia

[b]Department of Mathematics, Faculty of Applied Science,
Taiz University, Taiz, Yemen

E-Mail khaledma_sd@hotmail.com

Abstract

This article analyzes and compares the two algorithms for the numerical solutions of the fractional isothermal chemical equations (FICEs) based on mass action kinetics for autocatalytic feedback, involving the conversion of a reactant in the Liouville-Caputo sense. The first method is based upon the spectral collocation method (SCM), where the properties of Legendre polynomials are utilized to reduce the FICEs to a set of algebraic equations. We then use the well-known method like Newton-Raphson method (NRM) to solve the set of algebraic equations. The second method is based upon the properties of Newton polynomial interpolation (NPI) and the fundamental theorem of fractional calculus. We utilize these methods to construct the numerical solutions of the FICEs. The accuracy and effectiveness of these methods is satisfied graphically by combining the numerical results and plotting the absolute error. Also, the absolute errors are tabulated, and a good agreement found in all cases.

2020 Mathematics Subject Classification: 34A08; 35A22; 41A30; 65N22.

Key Words: Liouville-Caputo operator; fractional isothermal chemical; Legendre polynomials ; spectral collocation method; Newton polynomial interpolation; Newton-Raphson method.

1. Introduction

In the past few decades, the topic of the fractional differential equations has been the attention of many researchers and scientists. This is because many models related to the real world can't be modeled with classical differential equations. Therefore, the fractional differential equations can be used in simulation and modeling of many problems. For example in electrical, electronic, mechanical, biological and other areas of application related to the real world. For more details see [1, 2]. Unfortunately, it is difficult to find an exact solution for most of these models. As a result, the numerical and approximate methods have won the interest of many researchers. Using these methods, researchers were able to study and analyze the dynamic systems that govern these models. There are many such methods including, He's variational iteration method [3, 4], homotopy analysis [5, 6, 7], Fourier spectral methods [8], Adomian's decomposition method [9, 10], collocation methods [11, 12, 13, 14], finite difference schemes [15] and spectral methods[16, 17, 18, 19, 20, 21]. The model with three types of isothermal chemical reactions, this model is an extension of the model that Scott [22] and colleagues studied. The triple model includes three types of isothermal chemical reactions to include the thermal response capable of supporting complex periodic reactions as well as non-cyclical responses. The relatively stable reactant P is converted into a final product D through the chemical reaction of this model that contains three intermediate chemical species, U, V and W. These chemical reactions are

$$P \to U, \quad \text{rate} = k_0 p, \tag{1}$$

$$P + W \to U + W, \quad \text{rate} = k_w p w, \tag{2}$$

$$U \to V, \quad \text{rate} = k_a u, \tag{3}$$

$$U + 2V \to 3V, \quad \text{rate} = k_1 u v^2, \tag{4}$$

$$V \to W, \quad \text{rate} = k_2 V, \tag{5}$$

$$W \to D, \quad \text{rate} = k_3 w, \tag{6}$$

The governing rate equations for these reactions can be obtained by applying a mass action analysis to (1)–(6),

$$\frac{dp}{d\tau} = -k_0 p - k_w p w, \tag{7}$$

$$\frac{du}{d\tau} = k_0 p + k_w p w - k_a u - k_1 u v^2, \tag{8}$$

$$\frac{dv}{d\tau} = k_a u + k_1 u v^2 - k_2 v, \tag{9}$$

$$\frac{dw}{d\tau} = k_a u + k_1 u v^2 - k_2 v, \tag{10}$$

In dimensionless form, these equations are

$$\frac{d\beta_1}{dt} = -\alpha\beta_1(\vartheta + \beta_4), \tag{11}$$

$$\frac{d\beta_2}{dt} = \beta_1(\vartheta + \beta_4) - \beta_2\beta_3^2 - \beta_2, \tag{12}$$

$$\gamma\frac{d\beta_3}{dt} = \beta_2\beta_3^2 + \beta_2 - \beta_3, \tag{13}$$

$$\theta\frac{d\beta_4}{dt} = \beta_3 - \beta_4, \tag{14}$$

where

$$\beta_1 = \frac{k_c P}{k_3}, \quad \beta_2 = \left(\frac{k_1 k_u}{k_1^2}\right)^{\frac{1}{2}} a, \quad \beta_3 = \left(\frac{k_1}{k_4}\right)^{\frac{1}{2}}, \quad \beta_4 = \left(\frac{k_1 k_3^2}{k_4 k_2^2}\right)^{\frac{1}{2}}$$

are the dimensionless concentrations of the four chemical species and $t = k_a\tau$ is the dimensionless time. In addition, the dimensionless reaction rates are

$$\vartheta = \left(\frac{k_0 k_3}{k_2 k_c}\right)\left(\frac{k_1}{k_a}\right)^{\frac{1}{2}}, \quad \theta = \left(\frac{k_4}{k_3}\right), \quad \gamma = \left(\frac{k_a}{k_2}\right), \quad \alpha = \frac{k_w k_2}{k_3\left(k_1 k_a\right)^{\frac{1}{2}}}.$$

The importance and novelty of this work, it is to establish numerical approximate formulas in order to obtain numerical solutions for the proposed model of great importance in chemical applications. These formulas enable many researchers in applied sciences to benefit from them in studying the behavior and characteristics of these systems. After studying the accuracy of these numerical methods presented in this paper, a strong correlation can be made for the numerical results as well as the laboratory results. Also, the strong impetus for this study is that many fractional systems do not have exact solutions, so that the behavior of the solutions can be studied, and then the need to create schemes and iterative solutions is required.

In this section, we present the definitions and their properties that will be used in this work, [23, 24].

Definition 1. For $\lambda > 0$, and $\beta(t) \in L_1(a, b)$, with $L_1(a, b)$ the space of all integrable functions on (a, b), then the Riemann-Liouville fractional integral of order λ, denoted by J_0^λ, is given by

$$J_0^\lambda \beta(t) = \frac{1}{\Gamma(\lambda)} \int_0^t (t-\chi)^{\beta-1} \beta(\chi) d\chi. \tag{15}$$

Definition 2. For $\lambda > 0$, the Liouville-Caputo fractional derivative of order λ, denoted by ${}^{LC}D_0^\lambda$, is defined by

$$ {}^{\mathrm{LC}}{}_0\mathcal{D}_t^\lambda \beta(t) = \frac{1}{\Gamma(n-\lambda)} \int_0^t (t-\chi)^{n-\lambda-1} \mathcal{D}^n \beta(\chi) d\chi \tag{16}$$

$$(n-1 < \lambda < n;\ n \in \mathbb{N} = \{1, 2, 3, \cdots\}),$$

Replacing the derivatives $\frac{d}{dt}$ in the dimensionless chemical reaction equations (11)–(14) by the fractional derivatives ${}_0D_t^\lambda$, $0 < \lambda \leq 1$, $t > 0$, we obtain the fractional isothermal chemical model in the Liouville-Caputo sense as

$${}_0D_t^\lambda \beta_1(t) = -\alpha \beta_1(\vartheta + \beta_4), \tag{17}$$

$${}_0D_t^\lambda \beta_2(t) = \beta_1(\vartheta + \beta_4) - \beta_2\beta_3^2 - \beta_2, \tag{18}$$

$$\gamma_0 D_t^\lambda \beta_3(t) = \beta_2\beta_3^2 + \beta_2 - \beta_3, \tag{19}$$

$$\theta_0 D_t^\lambda \beta_4(t) = \beta_3 - \beta_4. \tag{20}$$

In this paper, the numerical scheme and solutions for the fractional isothermal chemical model in the Liouville-Caputo sense are constructed in the second and third sections. For the numerical results presented in the fourth section. The conclusion is presented in the fifth section.

2. Legendre spectral collocation method

Orthogonal functions play a very important role in the development of many numerical methods to address many real-world problems. Where by using the orthogonal functions, the solutions are approximated. By converting fractional differential models into a set of algebraic equations, then one of the known numerical methods is used to find an approximate solution to the resulting set of algebraic equations. By using well-known mathematical software, such as Mathematica or Matlab, we can easily find the Legendre coefficients, thereby creating numerical solutions of the fractional model presented in this paper (see [25] to [28]).

2.1. **Numerical Scheme and Its Convergence Analysis.** We begin by defining the shifted Legendre polynomials on the interval $[0,1]$ with the variable $z = 2t - 1$. These polynomials have the following property:

$$G_k(t) = G_k(2t-1) = G_{2k}(\sqrt{t}),$$

where the set $\{G_k(z) : k = 0, 1, 2, \cdots\}$ forms a family of orthogonal Legendre polynomials on the interval $[-1,1]$ (see, for details [29]). The analytic form of the shifted Legendre polynomials of degree s is given by

$$\bar{\mathbb{G}}_k(t) = \sum_{k=0}^{s} \frac{(-1)^{s+k}\,(s+k)!}{(k!)^2\,(s-k)!}\,t^k \qquad \left(\bar{\mathbb{G}}_0(t) = 1;\ \bar{\mathbb{G}}_1(t) = 2t-1;\ s = 2,3,4,\cdots\right). \tag{21}$$

The function $\beta(t) \in \mathcal{L}_2[0,1]$ can be expressed and approximated as a linear combination of the first $(m+1)$ terms of $\bar{\mathbb{G}}_k(t)$, as follows:

$$\beta(t) \simeq \beta_m(t) = \sum_{i=0}^{m} a_i\,\bar{\mathbb{G}}_k(t), \quad m = 1,2,3,4,\cdots, \tag{22}$$

where the coefficients a_i are given by

$$a_i = (2i+1)\int_0^1 \beta(t)\,\bar{\mathbb{G}}_k(t)\,dt \qquad (i = 0,1,2,\cdots).$$

Now, we state the following useful theorem.

Theorem 1. [30] *Let $\beta(t)$ be approximated by the shifted Legendre polynomials in* (22). *Suppose also that $\lambda > 0$. Then*

$$D^{\lambda}\beta(t) = \sum_{i=\lceil\lambda\rceil}^{m}\sum_{k=\lceil\lambda\rceil}^{i} a_i H_{i,k}^{(\lambda)} t^{k-\lambda}, \tag{23}$$

where

$$H_{i,k}^{(\lambda)} = \frac{(i+k)!\,\Gamma(k+1)}{(k!)^2\,(i-k)!\,\Gamma(k-\lambda+1)}.$$

2.2. **Construction the LSCM.** We will now implement the Legendre spectral collocation method to solve numerically the FICEs are given by (17)–(20) as follows [33]

$$\beta_{1,m}(t) = \sum_{k=0}^{m} \beta_{1,k}\,\bar{\mathbb{G}}_k(t), \qquad \beta_{2,m}(t) = \sum_{k=0}^{m} \beta_{2,k}\,\bar{\mathbb{G}}_k(t),$$

$$\beta_{3,m}(t) = \sum_{k=0}^{m} \beta_{3,k}\,\bar{\mathbb{G}}_k(t) \qquad \text{and} \qquad \beta_{4,m}(t) = \sum_{k=0}^{m} \beta_{4,k}\,\bar{\mathbb{G}}_k(t). \tag{24}$$

Substituting these expansions into the FICEs (17)–(20) and using (23), we obtain

$$\sum_{i=\lceil\lambda\rceil}^{m}\sum_{k=0}^{i-\lceil\lambda\rceil} \beta_{1,i}\,H_{i,k}^{(\lambda)}\,t^{i-k-\lambda} = -\alpha\left(\sum_{k=0}^{m}\beta_{1,i}\,\bar{\mathbb{G}}_k(t)\right)\left(\vartheta + \sum_{k=0}^{m}\beta_{4,i}\,\bar{\mathbb{G}}_k(t)\right), \tag{25}$$

$$\sum_{i=\lceil\lambda\rceil}^{m}\sum_{k=0}^{i-\lceil\lambda\rceil}\beta_{2,i}\,H_{i,k}^{(\lambda)}\,t^{i-k-\lambda}=\left(\sum_{k=0}^{m}\beta_{1,i}\,\bar{\mathbb{G}}_k(t)\right)\left(\vartheta+\sum_{k=0}^{m}\beta_{4,i}\,\bar{\mathbb{G}}_k(t)\right)-\left(\sum_{k=0}^{m}\beta_{2,i}\,\bar{\mathbb{G}}_k(t)\right)\left(\sum_{k=0}^{m}\beta_{3,i}\,\bar{\mathbb{G}}_k(t)\right)^2-\left(\sum_{k=0}^{m}\beta_{2,i}\,\bar{\mathbb{G}}_k(t)\right), \tag{26}$$

$$\sum_{i=\lceil\lambda\rceil}^{m}\sum_{k=0}^{i-\lceil\lambda\rceil}\beta_{3,i}\,H_{i,k}^{(\lambda)}\,t^{i-k-\lambda}=\left(\sum_{k=0}^{m}\beta_{2,i}\,\bar{\mathbb{G}}_k(t)\right)\left(\sum_{k=0}^{m}\beta_{3,i}\,\bar{\mathbb{G}}_k(t)\right)^2+\left(\sum_{k=0}^{m}\beta_{2,k}\,\bar{\mathbb{G}}_k(t)\right)-\left(\sum_{k=0}^{m}\beta_{3,i}\,\bar{\mathbb{G}}_k(t)\right), \tag{27}$$

$$\sum_{i=\lceil\lambda\rceil}^{m}\sum_{k=0}^{i-\lceil\lambda\rceil}\beta_{4,i}\,H_{i,k}^{(\lambda)}\,t^{i-k-\lambda}=\left(\sum_{k=0}^{m}\beta_{3,k}\,\bar{\mathbb{G}}_k(t)\right)-\left(\sum_{k=0}^{m}\beta_{4,i}\,\bar{\mathbb{G}}_k(t)\right). \tag{28}$$

The equations (25)–(28) are collocated at m nodes t_p, $p=0,1,\ldots,m-1$, as follows

$$\sum_{i=\lceil\lambda\rceil}^{m}\sum_{k=0}^{i-\lceil\lambda\rceil}\beta_{1,i}\,H_{i,k}^{(\lambda)}\,t_p^{i-k-\lambda}=-\alpha\left(\sum_{k=0}^{m}\beta_{1,i}\,\bar{\mathbb{G}}_k(t_p)\right)\left(\vartheta+\sum_{k=0}^{m}\beta_{4,i}\,\bar{\mathbb{G}}_k(t_p)\right), \tag{29}$$

$$\sum_{i=\lceil\lambda\rceil}^{m}\sum_{k=0}^{i-\lceil\lambda\rceil}\beta_{2,i}\,H_{i,k}^{(\lambda)}\,t_p^{i-k-\lambda}=\left(\sum_{k=0}^{m}\beta_{1,i}\,\bar{\mathbb{G}}_k(t_p)\right)\left(\vartheta+\sum_{k=0}^{m}\beta_{4,i}\,\bar{\mathbb{G}}_k(t_p)\right)-\left(\sum_{k=0}^{m}\beta_{2,i}\,\bar{\mathbb{G}}_k(t_p)\right)\left(\sum_{k=0}^{m}\beta_{3,i}\,\bar{\mathbb{G}}_k(t_p)\right)^2-\left(\sum_{k=0}^{m}\beta_{2,i}\,\bar{\mathbb{G}}_k(t_p)\right), \tag{30}$$

$$\sum_{i=\lceil\lambda\rceil}^{m}\sum_{k=0}^{i-\lceil\lambda\rceil}\beta_{3,i}\,H_{i,k}^{(\lambda)}\,t_p^{i-k-\lambda}=\left(\sum_{k=0}^{m}\beta_{2,i}\,\bar{\mathbb{G}}_k(t_p)\right)\left(\sum_{k=0}^{m}\beta_{3,i}\,\bar{\mathbb{G}}_k(t_p)\right)^2+\left(\sum_{k=0}^{m}\beta_{2,k}\,\bar{\mathbb{G}}_k(t_p)\right)-\left(\sum_{k=0}^{m}\beta_{3,i}\,\bar{\mathbb{G}}_k(t_p)\right), \tag{31}$$

$$\sum_{i=\lceil\lambda\rceil}^{m}\sum_{k=0}^{i-\lceil\lambda\rceil}\beta_{4,i}\,H_{i,k}^{(\lambda)}\,t_p^{i-k-\lambda}=\left(\sum_{k=0}^{m}\beta_{3,k}\,\bar{\mathbb{G}}_k(t_p)\right)-\left(\sum_{k=0}^{m}\beta_{4,i}\,\bar{\mathbb{G}}_k(t_p)\right). \tag{32}$$

In addition, the associated initial conditions can be obtained by using the expansions Eqs. (24). We thus have

$$\sum_{i=0}^{m}(-1)^i\,\beta_{1,i}=\beta_{1,0}, \tag{33}$$

$$\sum_{i=0}^{m}(-1)^i\,\beta_{2,i}=\beta_{2,0}, \tag{34}$$

$$\sum_{i=0}^{m}(-1)^i\,\beta_{3,i}=\beta_{3,0}, \tag{35}$$

$$\sum_{i=0}^{m}(-1)^i\,\beta_{4,i}=\beta_{4,0}. \tag{36}$$

Finally, using the Newton-Raphson iteration method, we can solve this system of algebraic equations and get the unknowns $\beta_{1,i},\ \beta_{2,i},\ \beta_{3,i},\ \beta_{4,i},\ i=0,1,\cdots,m$.

3. Newton polynomial interpolation

In this section, the numerical solutions of the proposed fractional system will be investigate, by establishing the iterative formulas, and employing them in finding the numerical solutions [34]. We apply the fundamental theorem of fractional calculus on (17)–(20) to obtain the following iterative formulas

$$\beta_1(t)-\beta_1(0)=\frac{1}{\Gamma(\lambda)}\int_0^t\Big(-\alpha\,\beta_1(\chi)(\vartheta+\beta_4(\chi))\Big)(t-\chi)^{\lambda-1}d\chi, \tag{37}$$

$$\beta_2(t)-\beta_2(0)=\frac{1}{\Gamma(\lambda)}\int_0^t\Big(\beta_1(\chi)(\vartheta+\beta_4(\chi))-\beta_2(\chi)\beta_3^2(\chi)-\beta_2(\chi)\Big)(t-\chi)^{\lambda-1}d\chi, \tag{38}$$

$$\beta_3(t)-\beta_3(0)=\frac{1}{\Gamma(\lambda)}\int_0^t\Big(\beta_2(\chi)\beta_3^2(\chi)+\beta_2(\chi)-\beta_3(\chi)\Big)(t-\chi)^{\lambda-1}d\chi, \tag{39}$$

$$\beta_4(t)-\beta_4(0)=\frac{1}{\Gamma(\lambda)}\int_0^t\Big(\beta_3(\chi)-\beta_4(\chi)\Big)(t-\chi)^{\lambda-1}d\chi. \tag{40}$$

These equations (37)–(40) can be reformulated as

$$\beta_1(t_{n+1})-\beta_1(0)=\frac{1}{\Gamma(\lambda)}\sum_{m=2}^{\infty}\int_{t_m}^{t_{m+1}}\Big(-\alpha\,\beta_1(\chi)(\vartheta+\beta_4(\chi))\Big)(t_{m+1}-\chi)^{\lambda-1}d\chi, \tag{41}$$

$$\begin{aligned}\beta_2(t_{n+1})-\beta_2(0)=&\frac{1}{\Gamma(\lambda)}\sum_{m=2}^{\infty}\int_{t_m}^{t_{m+1}}\Big(\beta_1(\chi)(\vartheta+\beta_4(\chi))-\beta_2(\chi)\beta_3^2(\chi)-\beta_2(\chi)\Big)\\&\times(t_{m+1}-\chi)^{\lambda-1}d\chi,\end{aligned} \tag{42}$$

$$\beta_3(t_{n+1})-\beta_3(0)=\frac{1}{\Gamma(\lambda)}\sum_{m=2}^{\infty}\int_{t_m}^{t_{m+1}}\Big(\beta_2(\chi)\beta_3^2(\chi)+\beta_2(\chi)-\beta_3(\chi)\Big)(t_{m+1}-\chi)^{\lambda-1}d\chi, \tag{43}$$

$$\beta_4(t_{n+1}) - \beta_4(0) = \frac{1}{\Gamma(\lambda)} \sum_{m=2}^{\infty} \int_{t_m}^{t_{m+1}} \Big(\beta_3(\chi) - \beta_4(\chi)\Big)(t_{m+1} - \chi)^{\lambda-1} d\chi. \tag{44}$$

Using Newton polynomial interpolation as in [35], we obtain

$$\begin{aligned}
\beta_1(t_{n+1}) &= \beta_1(0) + \frac{1}{\Gamma(\lambda)} \sum_{m=2}^{n} \Big(- \alpha\, \beta_1(t_{m-2})(\vartheta + \beta_4(t_{m-2}))\Big) \int_{t_m}^{t_{m+1}} \frac{1}{(t_{n+1} - \chi)^{1-\lambda}} d\chi \\
&+ \frac{1}{h\Gamma(\lambda)} \sum_{m=2}^{n} \Bigg(\Big(- \alpha\, \beta_1(t_{m-1})(\vartheta + \beta_4(t_{m-1}))\Big) \\
&- \Big(- \alpha\, \beta_1(t_{m-2})(\vartheta + \beta_4(t_{m-2}))\Big)\Bigg) \int_{t_m}^{t_{m+1}} \frac{(\chi - t_{m-2})}{(t_{n+1} - \chi)^{1-\lambda}} d\chi \\
&+ \frac{1}{2h^2\Gamma(\lambda)} \sum_{m=2}^{n} \Bigg(\Big(- \alpha\, \beta_1(t_m)(\vartheta + \beta_4(t_m))\Big) - 2\Big(- \alpha\, \beta_1(t_{m-1})(\vartheta + \beta_4(t_{m-1}))\Big) \\
&+ \Big(- \alpha\, \beta_1(t_{m-2})(\vartheta + \beta_4(t_{m-2}))\Big)\Bigg) \int_{t_m}^{t_{m+1}} \frac{(\chi - t_{m-2})(\chi - t_{m-1})}{(t_{n+1} - \chi)^{1-\lambda}} d\chi.
\end{aligned} \tag{45}$$

$$\begin{aligned}
\beta_2(t_{n+1}) &= \beta_2(0) + \frac{1}{\Gamma(\lambda)} \sum_{m=2}^{n} \Big(\beta_1(t_{m-2})(\vartheta + \beta_4(t_{m-2})) \\
&- \beta_2(t_{m-2})\beta_3^2(t_{m-2}) - \beta_2(t_{m-2})\Big) \int_{t_m}^{t_{m+1}} \frac{1}{(t_{n+1} - \chi)^{1-\lambda}} d\chi \\
&+ \frac{1}{h\Gamma(\lambda)} \sum_{m=2}^{n} \Bigg(\Big(\beta_1(t_{m-1})(\vartheta + \beta_4(t_{m-1})) - \beta_2(t_{m-1})\beta_3^2(t_{m-1}) - \beta_2(t_{m-1})\Big) \\
&- \Big(\beta_1(t_{m-2})(\vartheta + \beta_4(t_{m-2})) - \beta_2(t_{m-2})\beta_3^2(t_{m-2}) - \beta_2(t_{m-2})\Big)\Bigg) \\
&\times \int_{t_m}^{t_{m+1}} \frac{(\chi - t_{m-2})}{(t_{n+1} - \chi)^{1-\lambda}} d\chi \\
&+ \frac{1}{2h^2\Gamma(\lambda)} \sum_{m=2}^{n} \Bigg(\Big(\beta_1(t_m)(\vartheta + \beta_4(t_m)) - \beta_2(t_m)\beta_3^2(t_m) - \beta_2(t_m)\Big) \\
&- 2\Big(\beta_1(t_{m-1})(\vartheta + \beta_4(t_{m-1})) - \beta_2(t_{m-1})\beta_3^2(t_{m-1}) - \beta_2(t_{m-1})\Big) \\
&+ \Big(\beta_1(t_{m-2})(\vartheta + \beta_4(t_{m-2})) - \beta_2(t_{m-2})\beta_3^2(t_{m-2}) - \beta_2(t_{m-2})\Big)\Bigg) \\
&\times \int_{t_m}^{t_{m+1}} \frac{(\chi - t_{m-2})(\chi - t_{m-1})}{(t_{n+1} - \chi)^{1-\lambda}} d\chi.
\end{aligned} \tag{46}$$

$$\begin{aligned}
\beta_3(t_{n+1}) &= \beta_3(0) + \frac{1}{\Gamma(\lambda)}\sum_{m=2}^{n}\Big(\beta_2(t_{m-2})\beta_3^2(t_{m-2}) + \beta_2(t_{m-2}) - \beta_3(t_{m-2})\Big)\\
&\times \int_{t_m}^{t_{m+1}} \frac{1}{(t_{n+1}-\chi)^{1-\lambda}}d\chi\\
&+ \frac{1}{h\Gamma(\lambda)}\sum_{m=2}^{n}\Bigg(\Big(\beta_2(t_{m-1})\beta_3^2(t_{m-1}) + \beta_2(t_{m-1}) - \beta_3(t_{m-1})\Big)\\
&- \Big(\beta_2(t_{m-2})\beta_3^2(t_{m-2}) + \beta_2(t_{m-2}) - \beta_3(t_{m-2})\Big)\Bigg)\int_{t_m}^{t_{m+1}} \frac{(\chi - t_{m-2})}{(t_{n+1}-\chi)^{1-\lambda}}d\chi\\
&+ \frac{1}{2h^2\Gamma(\lambda)}\sum_{m=2}^{n}\Bigg(\Big(\beta_2(t_m)\beta_3^2(t_m) + \beta_2(t_m) - \beta_3(t_m)\Big)\\
&- 2\Big(\beta_2(t_{m-1})\beta_3^2(t_{m-1}) + \beta_2(t_{m-1}) - \beta_3(t_{m-1})\Big)\\
&+ \Big(\beta_2(t_{m-2})\beta_3^2(t_{m-2}) + \beta_2(t_{m-2}) - \beta_3(t_{m-2})\Big)\Bigg)\\
&\times \int_{t_m}^{t_{m+1}} \frac{(\chi - t_{m-2})(\chi - t_{m-1})}{(t_{n+1}-\chi)^{1-\lambda}}d\chi. \qquad (47)
\end{aligned}$$

$$\begin{aligned}
\beta_4(t_{n+1}) &= \beta_4(0) + +\frac{1}{\Gamma(\lambda)}\sum_{m=2}^{n}\Big(\beta_3(t_{m-2}) - \beta_4(t_{m-2})\Big)\int_{t_m}^{t_{m+1}} \frac{1}{(t_{n+1}-\chi)^{1-\lambda}}d\chi\\
&+ \frac{1}{h\Gamma(\lambda)}\sum_{m=2}^{n}\Bigg(\Big(\beta_3(t_{m-1}) - \beta_4(t_{m-1})\Big) - \Big(\beta_3(t_{m-2}) - \beta_4(t_{m-2})\Big)\Bigg)\\
&\times \int_{t_m}^{t_{m+1}} \frac{(\chi - t_{m-2})}{(t_{n+1}-\chi)^{1-\lambda}}d\chi\\
&+ \frac{1}{2h^2\Gamma(\lambda)}\sum_{m=2}^{n}\Bigg(\Big(\beta_3(t_m) - \beta_4(t_m)\Big) - 2\Big(\beta_3(t_{m-1}) - \beta_4(t_{m-1})\Big)\\
&+ \Big(\beta_3(t_{m-2}) - \beta_4(t_{m-2})\Big)\Bigg)\int_{t_m}^{t_{m+1}} \frac{(\chi - t_{m-2})(\chi - t_{m-1})}{(t_{n+1}-\chi)^{1-\lambda}}d\chi. \qquad (48)
\end{aligned}$$

The integrals in these Newton interpolation formulae are evaluated directly. The numerical solutions of (17)–(20) involving the LC derivative are then given by

$$\begin{aligned}
\beta_1(t_{n+1}) &= \beta_1(0) + \frac{h^\lambda}{\Gamma(1+\lambda)} \sum_{m=2}^{n} \Big(-\alpha\,\beta_1(t_{m-2})(\vartheta + \beta_4(t_{m-2}))\Big)\Lambda_1 \\
&+ \frac{h^\lambda}{\Gamma(2+\lambda)} \sum_{m=2}^{n} \Bigg(\Big(-\alpha\,\beta_1(t_{m-1})(\vartheta + \beta_4(t_{m-1}))\Big) \\
&- \Big(-\alpha\,\beta_1(t_{m-2})(\vartheta + \beta_4(t_{m-2}))\Big)\Bigg)\Lambda_2 \\
&+ \frac{h^\lambda}{2\Gamma(3+\lambda)} \sum_{m=2}^{n} \Bigg(\Big(-\alpha\,\beta_1(t_{m})(\vartheta + \beta_4(t_{m}))\Big) - 2\Big(-\alpha\,\beta_1(t_{m-1})(\vartheta + \beta_4(t_{m-1}))\Big) \\
&+ \Big(-\alpha\,\beta_1(t_{m-2})(\vartheta + \beta_4(t_{m-2}))\Big)\Bigg)\Lambda_3,
\end{aligned} \tag{49}$$

$$\begin{aligned}
\beta_2(t_{n+1}) &= \beta_2(0) + \frac{h^\lambda}{\Gamma(1+\lambda)} \sum_{m=2}^{n} \Big(\beta_1(t_{m-2})(\vartheta + \beta_4(t_{m-2})) \\
&- \beta_2(t_{m-2})\beta_3^2(t_{m-2}) - \beta_2(t_{m-2})\Big)\Lambda_1 \\
&+ \frac{h^\lambda}{\Gamma(2+\lambda)} \sum_{m=2}^{n} \Bigg(\Big(\beta_1(t_{m-1})(\vartheta + \beta_4(t_{m-1})) - \beta_2(t_{m-1})\beta_3^2(t_{m-1}) - \beta_2(t_{m-1})\Big) \\
&- \Big(\beta_1(t_{m-2})(\vartheta + \beta_4(t_{m-2})) - \beta_2(t_{m-2})\beta_3^2(t_{m-2}) - \beta_2(t_{m-2})\Big)\Bigg)\Lambda_2 \\
&+ \frac{h^\lambda}{2\Gamma(2+\lambda)} \sum_{m=2}^{n} \Bigg(\Big(\beta_1(t_{m})(\vartheta + \beta_4(t_{m})) - \beta_2(t_{m})\beta_3^2(t_{m}) - \beta_2(t_{m})\Big) \\
&- 2\Big(\beta_1(t_{m-1})(\vartheta + \beta_4(t_{m-1})) - \beta_2(t_{m-1})\beta_3^2(t_{m-1}) - \beta_2(t_{m-1})\Big) \\
&+ \Big(\beta_1(t_{m-2})(\vartheta + \beta_4(t_{m-2})) - \beta_2(t_{m-2})\beta_3^2(t_{m-2}) - \beta_2(t_{m-2})\Big)\Bigg)\Lambda_3,
\end{aligned} \tag{50}$$

$$\begin{aligned}
\beta_3(t_{n+1}) &= \beta_3(0) + \frac{h^\lambda}{\Gamma(1+\lambda)} \sum_{m=2}^{n} \Big(\beta_2(t_{m-2})\beta_3^2(t_{m-2}) + \beta_2(t_{m-2}) - \beta_3(t_{m-2})\Big)\Lambda_1 \\
&+ \frac{h^\lambda}{\Gamma(2+\lambda)} \sum_{m=2}^{n} \Bigg(\Big(\beta_2(t_{m-1})\beta_3^2(t_{m-1}) + \beta_2(t_{m-1}) - \beta_3(t_{m-1})\Big) \\
&- \Big(\beta_2(t_{m-2})\beta_3^2(t_{m-2}) + \beta_2(t_{m-2}) - \beta_3(t_{m-2})\Big)\Bigg)\Lambda_2 \\
&+ \frac{h^\lambda}{2\Gamma(3+\lambda)} \sum_{m=2}^{n} \Bigg(\Big(\beta_2(t_m)\beta_3^2(t_m) + \beta_2(t_m) - \beta_3(t_m)\Big) \\
&- 2\Big(\beta_2(t_{m-1})\beta_3^2(t_{m-1}) + \beta_2(t_{m-1}) - \beta_3(t_{m-1})\Big) \\
&+ \Big(\beta_2(t_{m-2})\beta_3^2(t_{m-2}) + \beta_2(t_{m-2}) - \beta_3(t_{m-2})\Big)\Bigg)\Lambda_3, \qquad (51)
\end{aligned}$$

$$\begin{aligned}
\beta_4(t_{n+1}) &= \beta_4(0) + \frac{h^\lambda}{\Gamma(1+\lambda)} \sum_{m=2}^{n} \Big(\beta_3(t_{m-2}) - \beta_4(t_{m-2})\Big)\Lambda_1 \\
&+ \frac{h^\lambda}{\Gamma(2+\lambda)} \sum_{m=2}^{n} \Bigg(\Big(\beta_3(t_{m-1}) - \beta_4(t_{m-1})\Big) - \Big(\beta_3(t_{m-2}) - \beta_4(t_{m-2})\Big)\Bigg)\Lambda_2 \\
&+ \frac{h^\lambda}{2\Gamma(3+\lambda)} \sum_{m=2}^{n} \Bigg(\Big(\beta_3(t_m) - \beta_4(t_m)\Big) - 2\Big(\beta_3(t_{m-1}) - \beta_4(t_{m-1})\Big) \\
&+ \Big(\beta_3(t_{m-2}) - \beta_4(t_{m-2})\Big)\Bigg)\Lambda_3 \qquad (52)
\end{aligned}$$

where

$$\Lambda_1 = (n-m+1)^\lambda - (n-m)^\lambda, \qquad (53)$$

$$\Lambda_2 = (n-m+1)^\lambda\Big((n-m+3+2\lambda) - (n-m+3+3\lambda)\Big), \qquad (54)$$

$$\begin{aligned}
\Lambda_3 &= (n-m+1)^\lambda\Big(2(n-m)^2 + (3\lambda+10)(n-m) + 2\lambda^2 + 9\lambda + 12\Big) \qquad (55) \\
&- (n-m)^\lambda\Big(2(n-m)^2 + (5\lambda+10)(n-m) + 6\lambda^2 + 18\lambda + 12\Big). \qquad (56)
\end{aligned}$$

4. Numerical Results and Discussion

In this section, the numerical results of the FICEs will be compared through the propped methods in this work. It will illustrate the comparison of numerical solutions through the figures and tables for different values of λ. Fig. 1(a)–(d) show the comparison of the numerical solutions of FICEs by two proposed methods for $\lambda = 1$, $m = 21$, $h = 0.003$, $L = 10$, $\alpha = 0.5$, $\vartheta = 0.1$, $\gamma = 0.05$ and $\theta = 2$. It can be seen that the from Fig. 1 that the two numerical solutions of FICEs agree in terms of behavior and their close to each other. In Fig. 2, the absolute errors between the two solutions are shown for the same parameter values as in Fig. 1. It is evident from this figure that the absolute error is very small and the error between the two solutions decreases with the use of more terms in the first method and the use of more iterations in the second method. In Figures 3 and 4 the calculations are repeated for the same values as in Figures 1 and 2 but in this case $\lambda = 0.8$ was set. This case is very important due it is the goal of this work, which is a comparative study of two different methods of the numerical solutions of FICEs. Also, we notice in these figures that the numerical solutions for the two methods are very close to each other and exhibit the same behavior. Also in the Tables 1-8, the numerical solutions are calculated using the two methods presented in this work. And the calculations of the absolute error in the case of the integer order and non-integer order for FICEs were done. From these tables we also note the accuracy and efficacy of numerical solutions, given the order of the absolute error, where, it ranges between 10^{-3} and 10^{-7}. The numerical results obtained in this paper agree with the numerical results obtained in [36].

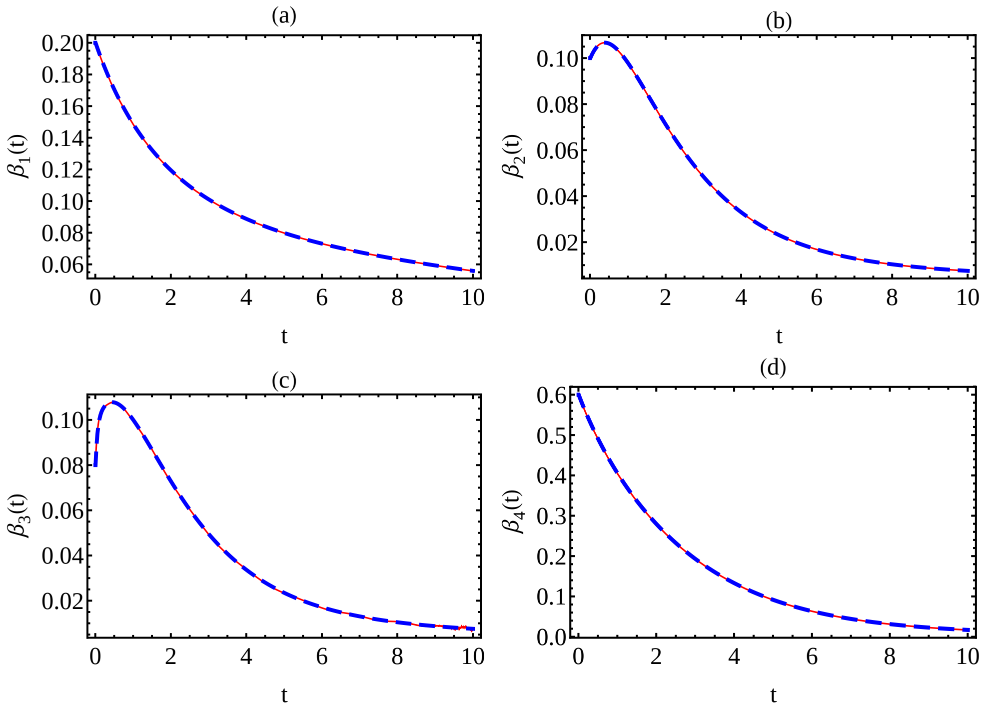

FIGURE 1. **Graph of the comparison between the numerical solutions for** $\alpha = 0.5, \vartheta = 0.1, \gamma = 0.05, \theta = 2, m = 21, h = 0.003, L = 10, \lambda = 1$**. (Blue dashed color: NPI; Red solid color: SCM)**

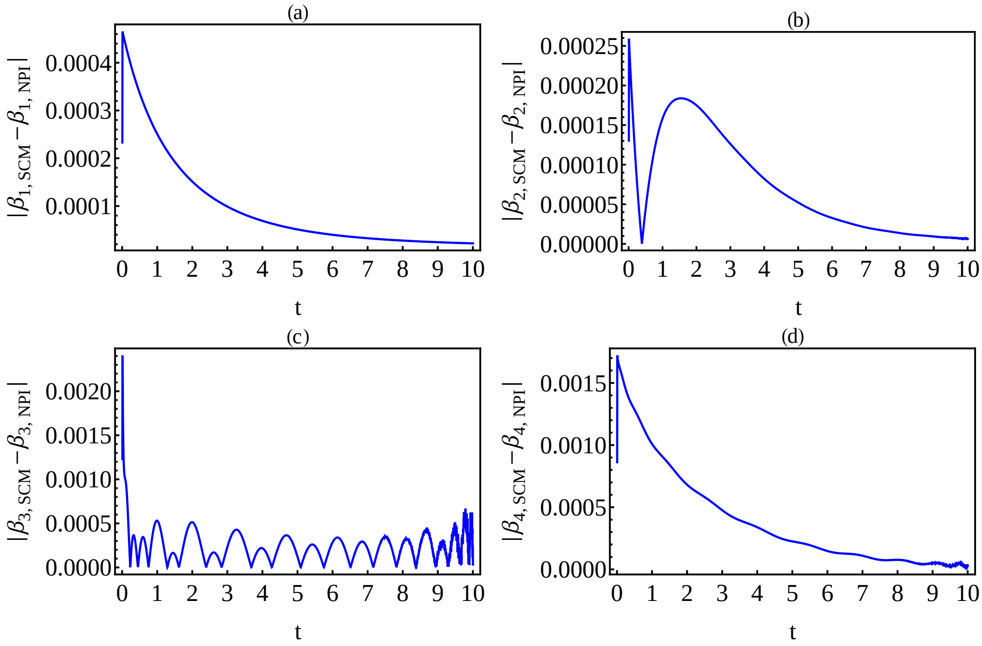

FIGURE 2. **Graph of the absolute error between the numerical solutions for** $\alpha = 0.5, \vartheta = 0.1, \gamma = 0.05, \theta = 2, m = 21, h = 0.003, L = 10, \lambda = 1$

n	$\beta_{1,SCM}(t)$	$\beta_{1,NPI}$	$\lvert\beta_{1,SCM}(t) - \beta_{1,NPI}\rvert$
0	0.2	0.2	3.19162×10^{-18}
200	0.162359	0.162662	3.03478×10^{-4}
400	0.137154	0.137364	2.09480×10^{-4}
600	0.119369	0.11952	1.51060×10^{-4}
800	0.106315	0.106428	1.12920×10^{-4}
1000	0.0964151	0.096502	8.69248×10^{-5}
1200	0.0886838	0.0887527	6.88986×10^{-5}
1400	0.0824808	0.0825367	5.59788×10^{-5}
1600	0.0773756	0.0774223	4.66744×10^{-5}
1800	0.073073	0.0731128	3.97719×10^{-5}
2000	0.0693664	0.0694011	3.46306×10^{-5}
2200	0.0661096	0.0661403	3.07003×10^{-5}
2400	0.0631978	0.0632255	2.76781×10^{-5}
2600	0.0605554	0.0605807	2.52558×10^{-5}
2800	0.0581273	0.0581506	2.33462×10^{-5}
3000	0.0558729	0.0558947	2.17804×10^{-5}

TABLE 1. **The absolute error between the numerical solutions for** $\alpha = 0.5, \vartheta = 0.1, \gamma = 0.05, \theta = 2, m = 21, h = 0.003, L = 10, \lambda = 1.$

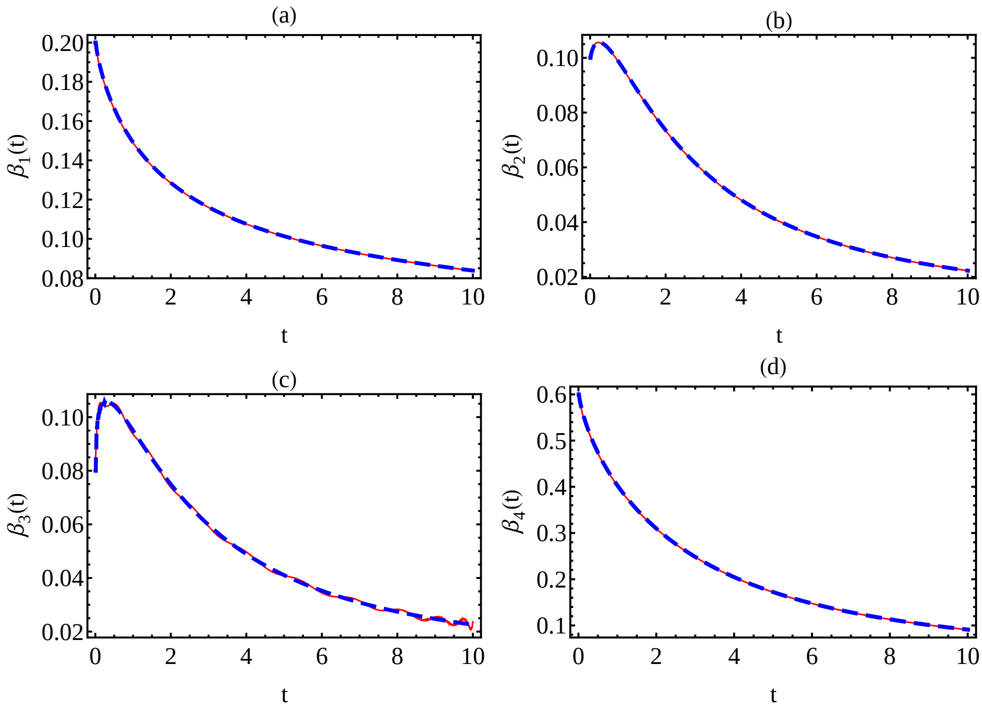

FIGURE 3. **Graph of the comparison between the numerical solutions for** $\alpha = 0.05, \vartheta = 2, \gamma = 0.05, \theta = 0.2, m = 21, h = 0.003, L = 10, \lambda = 0.8$. **(Blue dashed color: NPI; Red solid color: SCM)**

n	$\beta_{2,SCM}(t)$	$\beta_{2,NPI}$	$\lvert\beta_{2,SCM}(t) - \beta_{2,NPI}\rvert$
0	0.1	0.1	6.64074×10^{-19}
200	0.104424	0.104521	9.68429×10^{-5}
400	0.0891975	0.0893786	1.81056×10^{-4}
600	0.0710369	0.0712117	1.74852×10^{-4}
800	0.0550999	0.0552427	1.42801×10^{-4}
1000	0.0424772	0.0425876	1.1044×10^{-4}
1200	0.0329242	0.0330062	8.20209×10^{-4}
1400	0.0258433	0.025904	6.07221×10^{-4}
1600	0.02064	0.0206844	4.44039×10^{-5}
1800	0.0168194	0.0168521	3.26876×10^{-5}
2000	0.014003	0.0140272	2.42145×10^{-5}
2200	0.0119112	0.0119292	1.80192×10^{-5}
2400	0.0103409	0.0103545	1.36329×10^{-5}
2600	0.00914671	0.00915729	1.05799×10^{-5}
2800	0.00822487	0.00823305	8.1831×10^{-6}
3000	0.00750075	0.00750716	6.41186×10^{-6}

TABLE 2. **The absolute error between the numerical solutions for** $\alpha = 0.5, \vartheta = 0.1, \gamma = 0.05, \theta = 2, m = 21, h = 0.003, L = 10, \lambda = 1$.

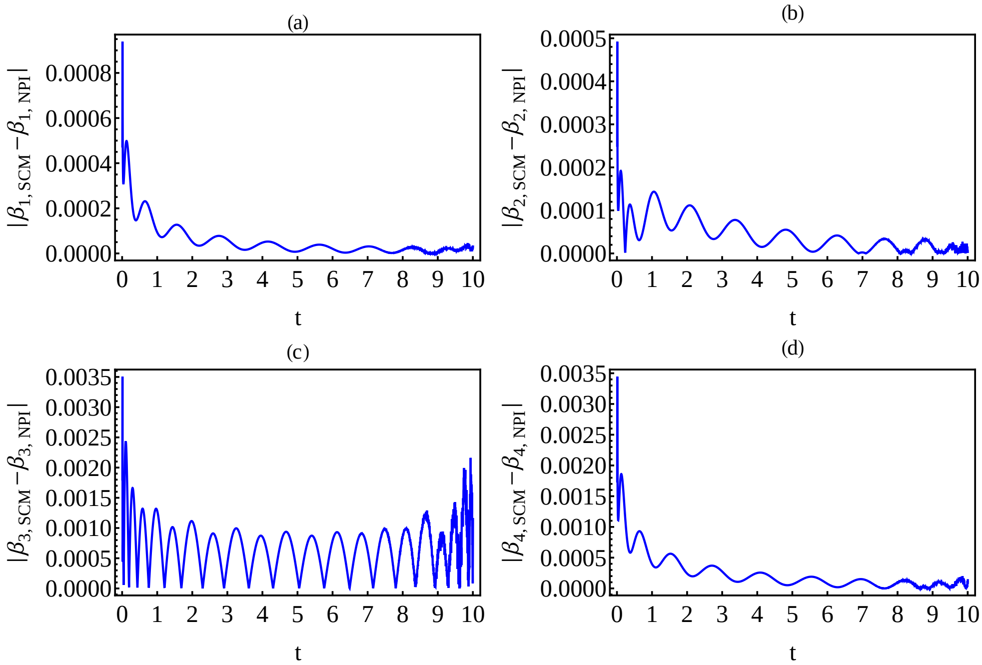

FIGURE 4. **Graph of the absolute error between the numerical solutions for** $\alpha = 0.05, \vartheta = 2, \gamma = 0.05, \theta = 0.2, m = 21, h = 0.003, L = 10, \lambda = 0.8$.

n	$\beta_{3,SCM}(t)$	$\beta_{3,NPI}$	$\lvert\beta_{3,SCM}(t) - \beta_{3,NPI}\rvert$
0	0.08	0.08	6.93889×10^{-18}
200	0.106587	0.106335	2.51509×10^{-4}
400	0.0915829	0.0915039	7.90304×10^{-5}
600	0.0724219	0.0729348	5.12911×10^{-4}
800	0.0566815	0.0565243	1.57174×10^{-4}
1000	0.0431098	0.0435182	4.08387×10^{-4}
1200	0.033895	0.0336778	2.17171×10^{-4}
1400	0.0260243	0.026389	3.64716×10^{-4}
1600	0.0212759	0.0210359	2.3997×10^{-4}
1800	0.0168213	0.0171086	2.87229×10^{-4}
2000	0.0144162	0.014216	2.00189×10^{-4}
2200	0.0118207	0.0120696	2.48862×10^{-4}
2400	0.0107311	0.0104603	2.7080×10^{-4}
2600	0.00881768	0.00923811	420430×10^{-4}
2800	0.00813945	0.00829586	1.56405×10^{-4}
3000	0.00759008	0.00755687	3.32133×10^{-5}

TABLE 3. **The absolute error between the numerical solutions for** $\alpha = 0.5, \vartheta = 0.1, \gamma = 0.05, \theta = 2, m = 21, h = 0.003, L = 10, \lambda = 1$.

n	$\beta_{4,SCM}(t)$	$\beta_{4,NPI}$	$\lvert\beta_{4,SCM}(t) - \beta_{4,NPI}\rvert$
0	0.6	0.6	7.24247×10^{-17}
200	0.459588	0.460777	1.18848×10^{-3}
400	0.357414	0.358309	8.94975×10^{-4}
600	0.279207	0.279887	6.80213×10^{-4}
800	0.218143	0.218691	5.47852×10^{-4}
1000	0.17028	0.170696	4.15683×10^{-4}
1200	0.132766	0.133105	3.38834×10^{-4}
1400	0.103528	0.103778	2.49804×10^{-4}
1600	0.0807937	0.0810007	2.06965×10^{-4}
1800	0.063239	0.0633866	1.47547×10^{-4}
2000	0.0496907	0.0498149	1.2425×10^{-4}
2200	0.0393028	0.0393879	8.50452×10^{-5}
2400	0.0313156	0.0313926	7.6974×10^{-5}
2600	0.0252256	0.0252684	4.27996×10^{-5}
2800	0.0205407	0.0205778	3.70776×10^{-5}
3000	0.0169492	0.0169816	3.24183×10^{-5}

TABLE 4. **The absolute error between the numerical solutions for** $\alpha = 0.5, \vartheta = 0.1, \gamma = 0.05, \theta = 2, m = 21, h = 0.003, L = 10, \lambda = 1$.

n	$\beta_{1,SCM}(t)$	$\beta_{1,NPI}$	$\lvert\beta_{1,SCM}(t) - \beta_{1,NPI}\rvert$
0	0.2	0.2	6.071532×10^{-18}
200	0.159387	0.159618	2.30538×10^{-4}
400	0.140645	0.140746	1.00463×10^{-4}
600	0.128397	0.128448	5.08711×10^{-5}
800	0.119538	0.119614	7.53509×10^{-5}
1000	0.112869	0.112891	2.21489×10^{-5}
1200	0.107517	0.107565	4.81515×10^{-5}
1400	0.103194	0.103212	1.81214×10^{-5}
1600	0.0995369	0.0995646	2.77116×10^{-5}
1800	0.0964235	0.0964438	2.03372×10^{-5}
2000	0.093711	0.0937263	1.52962×10^{-5}
2200	0.0913054	0.091324	1.85645×10^{-5}
2400	0.0891566	0.0891726	1.59665×10^{-5}
2600	0.0872193	0.0872242	4.89773×10^{-6}
2800	0.0854236	0.0854423	1.86806×10^{-5}
3000	0.0837683	0.0837989	3.06043×10^{-5}

TABLE 5. **The absolute error between the numerical solutions for** $\alpha = 0.5, \vartheta = 0.1, \gamma = 0.05, \theta = 2, m = 21, h = 0.003, L = 10, \lambda = 0.8$.

n	$\beta_{2,SCM}(t)$	$\beta_{2,NPI}$	$\lvert\beta_{2,SCM}(t)-\beta_{2,NPI}\rvert$
0	0.1	0.1	2.168404×10^{-18}
200	0.100177	0.10021	3.34464×10^{-5}
400	0.0862051	0.0862899	8.48489×10^{-5}
600	0.0734054	0.0735147	1.09363×10^{-5}
800	0.0630386	0.0630745	3.59705×10^{-5}
1000	0.0546495	0.0547271	7.75792×10^{-5}
1200	0.0480308	0.0480499	1.91111×10^{-5}
1400	0.0426172	0.0426683	5.1118×10^{-5}
1600	0.0382718	0.0382874	1.56726×10^{-5}
1800	0.0346542	0.0346832	2.90497×10^{-5}
2000	0.0316701	0.0316866	1.64846×10^{-5}
2200	0.029152	0.0291699	1.7855×10^{-5}
2400	0.0270286	0.0270359	7.23923×10^{-6}
2600	0.0251817	0.02521	2.82558×10^{-5}
2800	0.0236307	0.0236344	3.72900×10^{-6}
3000	0.0222676	0.0222641	3.52774×10^{-6}

TABLE 6. **The absolute error between the numerical solutions for** $\alpha=0.5,\vartheta=0.1,\gamma=0.05,\theta=2,m=21,h=0.003,L=10,\lambda=0.8$.

n	$\beta_{3,SCM}(t)$	$\beta_{3,NPI}$	$\lvert\beta_{3,SCM}(t)-\beta_{3,NPI}\rvert$
0	0.08	0.08	3.469447×10^{-18}
200	0.102461	0.101539	9.22728×10^{-4}
400	0.088632	0.0878293	8.02756×10^{-4}
600	0.0737625	0.0748701	1.10762×10^{-3}
800	0.0650606	0.0642195	8.41055×10^{-4}
1000	0.0547668	0.0556929	926154×10^{-4}
1200	0.0497238	0.0488716	8.52278×10^{-4}
1400	0.0424371	0.0433749	9.37781×10^{-4}
1600	0.0397346	0.0389017	8.32905×10^{-4}
1800	0.0344243	0.0352226	7.9836×10^{-4}
2000	0.0328434	0.0321648	6.78616×10^{-4}
2200	0.0288634	0.0295975	7.34043×10^{-4}
2400	0.0282892	0.0274212	8.68008×10^{-4}
2600	0.0243502	0.0255596	1.20941×10^{-3}
2800	0.0234221	0.0239537	5.31656×10^{-4}
3000	0.0237056	0.0225574	1.14814×10^{-3}

TABLE 7. **The absolute error between the numerical solutions for** $\alpha=0.5,\vartheta=0.1,\gamma=0.05,\theta=2,m=21,h=0.003,L=10,\lambda=0.8$.

n	$\beta_{4,SCM}(t)$	$\beta_{4,NPI}$	$\lvert\beta_{4,SCM}(t) - \beta_{4,NPI}\rvert$
0	0.6	0.6	7.806256×10^{-18}
200	0.445779	0.446702	922925×10^{-4}
400	0.365854	0.366332	4.77962×10^{-4}
600	0.309166	0.309406	2.39652×10^{-4}
800	0.265732	0.2661	3.68341×10^{-4}
1000	0.231844	0.231963	1.18446×10^{-4}
1200	0.204193	0.204444	2.51442×10^{-4}
1400	0.181822	0.181901	7.94219×10^{-4}
1600	0.163035	0.163197	1.61688×10^{-4}
1800	0.147437	0.147512	7.43729×10^{-5}
2000	0.134137	0.134236	9.88674×10^{-5}
2200	0.122846	0.122905	5.93385×10^{-5}
2400	0.113066	0.113162	9.57111×10^{-5}
2600	0.104737	0.104725	1.24414×10^{-5}
2800	0.0973151	0.0973716	5.65149×10^{-5}
3000	0.0907919	0.0909248	1.32908×10^{-4}

Table 8. **The absolute error between the numerical solutions for** $\alpha = 0.5, \vartheta = 0.1, \gamma = 0.05, \theta = 2, m = 21, h = 0.003, L = 10, \lambda = 0.8$.

5. Conclusion

In this paper, two numerical methods are presented to evaluate the numerical solutions of the fractional isothermal chemical equations. The first method is based on the use of the properties of Legendr polynomial and collocation method. Whereas the second method is constructed with Newton polynomial interpolation and the fundamental theorem of fractional calculus. These two methods were employed to find numerical solutions for the fractional isothermal chemical equations. The numerical solutions were compared using the two methods presented by combining the solutions together, as well as calculating the amount of absolute error between the numerical solutions. This is illustrated by means of figures and tables, found to be good compatibility, and the order of the error is very small. All the numerical solutions obtained by using the computer program package *Mathematica*. This study gives us a good impression that it can be applied to many fractional differential models, as well as to more than one variable.

This research can be extended so that, we can focus on using fractional space-time derivatives on isothermal chemical equations. It is also possible to re-study this research in case the fractional-order as a time-varying function.

Conflicts of Interest: The author declares that he has no conflicts of interest.

References

[1] R. Caponetto and G. Dongola and L. Fortuna and I. PetráS, Fractional order systems: modeling and control applications,World Scientific, 2010

[2] M. A. Concepción, Y. ChenBlas, B. M. Vinagre, X. VinagreDingyü, F. Vicente, Fractional-order Systems and Controls , Springer, London, 2010 ,doi.org/10.1007/978-1-84996-335-0.

[3] J. H. He, Variational iteration method-a kind of nonlinear analytical technique: some examples. Int. J. Non-Linear Mech. 34(1999) 708–799.

[4] K. M. Saad, E. H. F Al-Sharif Analytical study for time and time-space fractional Burgers equation Advances in Difference Equations 2017 (1)(2017) 300.

[5] S.-J. Liao. On the homotopy analysis method for nonlinear problems. Appl. Math. Comput. 147(2004) 499–513.

[6] K. M. Saad, E. H. F AL-Shareef, A. K. Alomari, D. Baleanu, J. F. Gmez-Aguilar, On exact solutions for timefractional Korteweg-de Vries and Korteweg-de Vries-Burgers equations using homotopy analysis transform method, Chinese Journal of Physics 63(2020) 149–162.

[7] A. K. Alomari, T. Abdeljawad, D. Baleanu , K. M. Saad, Q. M. Al-Mdallal,, Numerical solutions of fractional parabolic equations with generalized MittagLeffler kernels *Numerical Methods for Partial Differential Equations*, (2020), doi.org/10.1002/num.22699.

[8] A. Bueno-Orovio, D. Kay, K. Burrage, Fourier spectral methods for fractional-in-space reaction-diffusion equations, Bit Numer Math 54(2014) 937–954.

[9] X. C. Shi, L. L. Huang, Y. Zeng, Fast Adomian decomposition method for the Cauchy problem of the time-fractional reaction diffusion equation. Adv. Mech. Eng. 8(2), 1-5 (2016)

[10] H. M. Srivastava, K. M. Saad , New approximate solution of the time-fractional Nagumo equation involving fractional integrals without singular kernel , Appl. Math. Inf. Sci 14(1)(2020) 1–8.

[11] Y Šocel, K. Yildiray, K. Aydin: The solution of the Bagley Torvik equation with the generalized Taylor collocation method. J. Franklin Inst. 347(2)(2010) 452–466.

[12] M. M. Khader, K. M. Saad, D. Baleanu, S. Kumar, A spectral collocation method for fractional chemical clock reactions, *Computational and Applied Mathematics* **39**(2020), 324.

[13] H. M. Srivastava K. M. Saad, M. M. Khader, An efficient spectral collocation method for the dynamic simulation of the fractional epidemiological model of the Ebola virus, *Chaos, Solitons & Fractals* **140**(2020), 110174.

[14] M. M. Khader, K. M.Saad, Z. Hammouch, A spectral collocation method for solving fractional KdV and KdV-Burgers equations with non-singular kernel derivatives, *Applied Numerical Mathematics* **161**(2021), 137–146.

[15] Y. Takeuchi, Y. Yoshimoto, R. Suda: Second order accuracy finite difference methods for space-fractional partial differential equations. J. Comput. Appl. Math. 320(2017)101-119.

[16] H. Singh, A. Wazwaz, Computational Method for Reaction Diffusion-Model Arising in a Spherical Catalyst, *International Journal of Applied and Computational Mathemati* **7(3)** (2021), 65.

[17] H. Singh, A new stable algorithm for fractional Navier-Stokes equation in polar coordinate, *International Journal of Applied and Computational Mathematics* **4** (2017), 3705–3722.

[18] H. Singh, Jacobi collocation method for the fractional advection-dispersion equation arising in porous media, Numerical methods for partial differential equations, *Numerical methods for partial differential equations*, (2020), doi.org/10.1002/num.22674.

[19] H. Singh, Jacobi collocation method for the fractional advection-dispersion equation arising in porous media, *International journal of dynamic and control*, (2021), 463–474.

[20] H. Singh H. M. Srivastava, D. Kumar, A reliable algorithm for the approximate solution of the nonlinear Lane-Emden type equations arising in astrophysics, *Numerical Methods for Partial Differential Equations* **34 (5)** (2018), 1524–1555.

[21] H. Singh, Analysis of drug treatment of the fractional HIV infection model of CD4+ T-cells, *Chaos, Solitons & Fractals* **146** (2021), 110868.

[22] S. K. Scott, Transient chaos in a closed chemical system, J. Chem. Phys. 94 (1991) 1134, https://doi.org/10.1063/1.460019

[23] A. A. Kilbas, H. M. Srivastava and J. J. Trujillo, Theory and Applications of Fractional Differential Equations, North-Holland Mathematical Studies, 204, Elsevier (North-Holland) Science Publishers, Amsterdam, London and New York, 2006.

[24] I. Podlubny, Fractional Differential Equations. Academic Press, New York(1993)

[25] H. Khalil, R. A. Khan, M. H. Al-Smadi, A. A. Freihat and N. Shawagfeh, New Operational matrix for shifted Legendre polynomials and fractional differential equations with variable coefficients , *Punjab Univ. J. Math.* **47** (2015), 1–23.

[26] F. Mohammadi and C. Cattani, A generalized fractional-order Legendre wavelet Tau method for solving fractional differential equations, *J. Comput. Appl. Math.* **339** (2018), 306–316.

[27] F. Mohammadi and S. T. Mohyud-Din, A fractional-order Legendre collocation method for solving the Bagley-Torvik equations, *Punjab Univ. J. Math.* **269** (2016), 2–14.

[28] H. M. Srivastava, K. M. Saad, Comparative Study of the Fractional-Order Clock Chemical Model. *Mathematics* **8** (2020), 1436.

[29] N. N. Lebedev, *Special Functions and Their Applications* (Translated from the Russian by R. A. Silverman), Prentice-Hall Incorporated, Englewood Cliffs, New Jersey, 1965; Dover Publications, New York, 1972.

[30] M. M. Khader and A. S. Hendy, The approximate and exact solutions of the fractional-order delay differential equations using Legendre pseudo-spectral method, *Internat. J. Pure Appl. Math.* **74** (2012), 287–297.

[31] K. M. Saad, New fractional derivative with non-singular kernel for deriving Legendre spectral collocation method, Alexandria Engineering Journal, 59(4)(2020) 1909–1917.

[32] M. M. Khader and K. M. Saad, A numerical approach for solving the problem of biological invasion (fractional Fisher equation) using Chebyshev spectral collocation method, Chaos Solitons Fractals 110(2018)169–177.

[33] N. H. Sweilam, A. M. Nagy, A. A. El-Sayed, Second kind shifted Chebyshev polynomials for solving space fractional order diffusion equation, Chaos, Solitons & Fractals 73(2015) 141–147.

[34] K. M. Owolabi, A. Atangana, Numerical Simulation of Noninteger Order System in Subdiffusive, Diffusive, and Superdiffusive Scenarios, Journal of Computational and Nonlinear Dynamics. 12(3)(2017) 1–7.

[35] A. Atangana S. I. Araz, New Numerical Scheme with Newton Polynomial,Theory, Methods, and Applications, (2021).

[36] K. M.Saad, Comparative study on Fractional Isothermal Chemical Model, *Alexandria Engineering Journal*, **60(3)** (2021), 3265–3274.